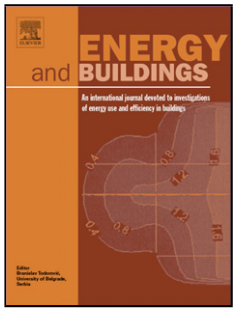

Title: Experimental and numerical analysis of the influence of inlet configuration on the performance of a roof top solar chimney

Authors: Hussain H. Al-Kayiem, K.V. Sreejaya, Aja O. Chikere

PII: S0378-7788(17)31657-2
DOI: https://doi.org/10.1016/j.enbuild.2017.10.063
Reference: ENB 8083

To appear in: *ENB*

Received date: 10-5-2017
Revised date: 1-10-2017
Accepted date: 18-10-2017

Please cite this article as: Hussain H.Al-Kayiem, K.V.Sreejaya, Aja O.Chikere, Experimental and numerical analysis of the influence of inlet configuration on the performance of a roof top solar chimney, Energy and Buildings https://doi.org/10.1016/j.enbuild.2017.10.063

Experimental and Numerical Analysis of the Influence of Inlet Configuration on the Performance of a Roof Top Solar Chimney

Hussain H. Al-Kayiem[1,*], Sreejaya K.V.[1], and Aja O. Chikere[2]

[1] Mechanical Engineering Department, Universiti Teknologi PETRONAS, 32610 Bandar Seri Iskandar, Malaysia

[2] Mechanical Engineering Department, Curtin University, 98009 Miri, Sarawak, Malaysia

[*]email: hussain_kayiem@utp.edu.my

Graphical abstract

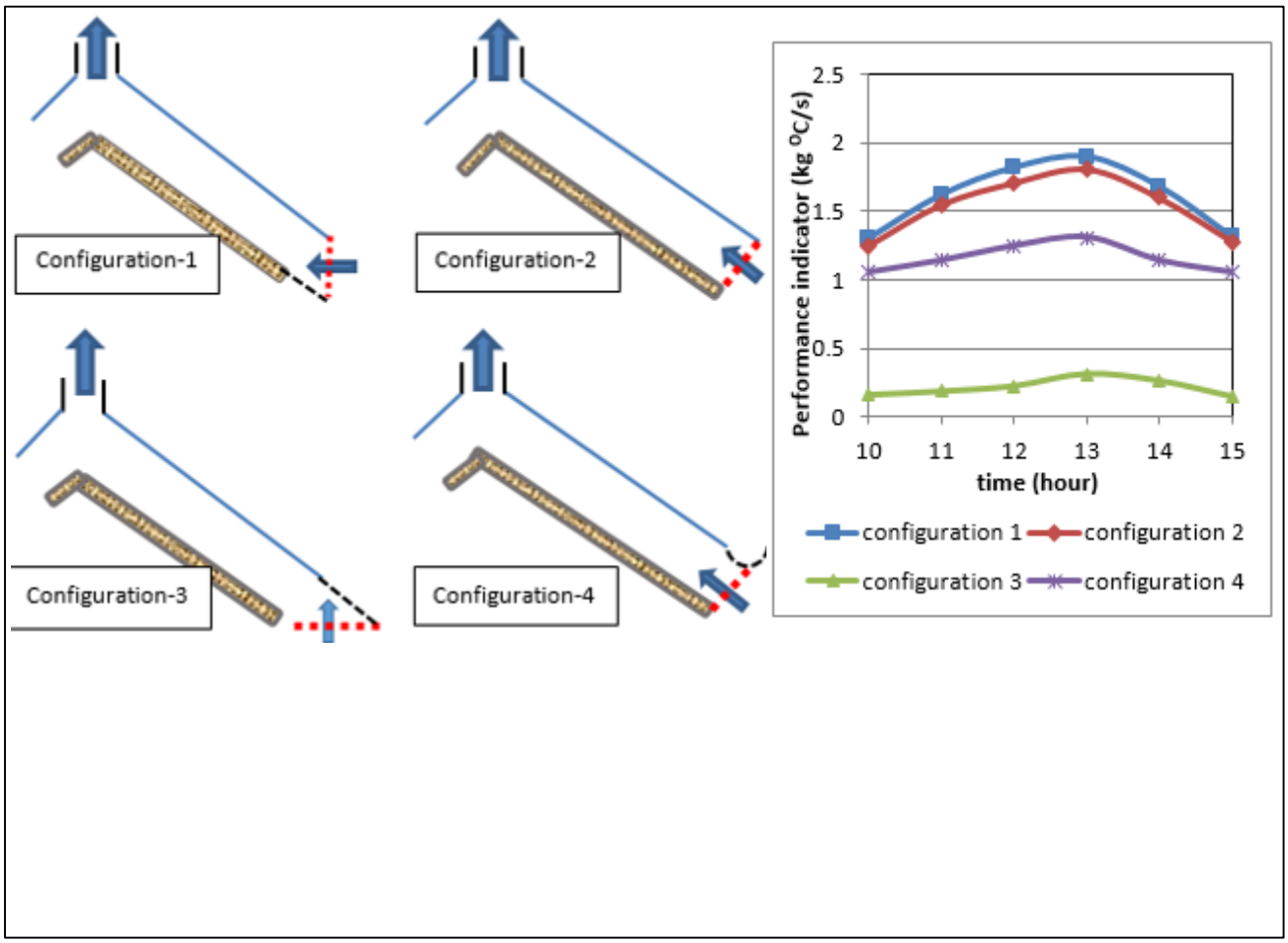

Four different configurations of collector inlet of a Roof top solar chimney have been investigated experimentally and numerically. The results demonstrated that configuration 1, with vertical cross section is superior compared to the other types. The CFD simulation showed that the air particles are moving from the upper zone and inters to the collector passage. Hence, it is recommended for any solar natural convection air heating system to be designed with vertical cross section inlet

Highlights

- Experimental model of RTSC has been designed, fabricated and evaluated with four different inlet configurations.
- Numerical model of RTSC has been developed and the simulation results have been presented as velocity vector contours.
- The performance of the RTSC is identified using the mass flow rate X air temperature rise, as performance indicator.
- Experimental and numerical results of four different types of inlet configurations have been compared and discussed.

Abstract

The Roof Top Solar Chimney system is a natural solar updraft technique utilizing the solar energy to generate wind stream within the system passage that has enough driving force to create stack effect. The influence of the inlet shape of the solar air collector on the solar chimney performance was investigated experimentally and numerically in the present paper. Four different inlet configurations have been modeled and ANSYS FLUENT software was used to simulate and visualize the 2-D aero-thermal flow field surrounding the inlet region. Experimental measurements of the four different inlets were conducted using a roof top solar chimney set up to validate the simulation results and to evaluate and compare the system performance at each inlet configuration. The experimental model has two identical transparent covers installed over the roof of a room model, opened at the top to allow air flow from both sides to a chimney pipe. It was found that when the inlet has vertical cross section, it offered the best performance as the velocity and mass flow rate of the air at the chimney was observed to be higher compared with the other three inlet configurations. When the inlet cross section was employed as horizontal, the performance of the collector was reduced by 84% compared to the vertical inlet setting, at 1.00pm. The CFD analysis demonstrated, interestingly, that most of the air flow in the collector was directed from upper region above the inlet, while small amount is flowing from the bottom side of the inlet. This justify the reason of very low performance of air solar collector with horizontal orientation. The results revealed the possibility of reducing the area of the transparent canopy of the solar chimney power plant and convert the outer region to open top absorber.

Keywords- energy conversion; roof top solar chimney; flow inlet; solar air heater; solar chimney; solar updraft.

1. INTRODUCTION

Natural ventilation is an attractive feature in the recent direction of green and low energy buildings, where it could reduce the carbon footprint and the CO_2 emission by reducing the electric consumption. Natural ventilation may be achieved by the roof top solar chimney (RTSC) technique, where the roof of the building is utilized as inclined solar absorber. A translucent sheet covers the absorber and allows the penetration of solar radiation which heats up the absorber. The simple combination of the absorber and the cover acts as a solar air collector which creates greenhouse environment inside the collector passage. In some designs, ambient air enters to the created greenhouse environment and gain thermal energy, by natural convection heat transfer from the absorber and converted to kinetic energy and flow up to the top of the air collector, where a short chimney is installed to enhance the stack effect. In some other designs, room air is guided into the gap between the absorber and the transparent cover.

The RTSC was studied experimentally, and simulated mathematically and numerically by many previous researchers. Research works are focused on evaluation of the system performance at various design and operation parameters. The issue of the gap size, which is the distance between the absorber and the transparent cover, represents a major target of many research works. As pointed by da Silva and Gosselin [1], the existence of an optimal spacing between the vertical wall stems is based on the fact that when gap-to-height ratio is small enough, the fluid reaches a temperature of the order of wall temperature before the end of channel, and consequently, heat transfer in the upper part of channel becomes to be very small. Contrary, when the gap-to-height ratio is large, thermal boundary-layer regime takes place. Hence, heat transfer keeps taking place up to the top of the channel due to difference in the bulk fluid temperature and the wall temperature. Consequently, wall-to-wall spacing needs to be optimized.

Ong (2003) [2] proposed a simple mathematical model of steady state heat transfer in a RTSC. Then, Ong and Chow (2003) [3] validated the mathematical model by comparison with experimental results. Focus was made on the effect of the solar intensity and the air gap between the glass cover and the absorber wall. They have investigated 0.1, 0.2, and 0.3 m air gap and claimed that there was no reverse flow in the chimney even with large gap of 0.3 m. Other investigator reported more information in terms of gap-to-height ratio.

Zamora and Kaiser 2009, [4] studied, through numerical investigation, the laminar and turbulent flows induced by natural convection in channels, with side wall solar chimney configuration, for a wide range of Rayleigh number and several values of the relative wall-to-wall spacing. The open from the room to the chimney gap is located at the bottom. They recommended an optimum gap-to-height ratio in correlation format, as function of Ra number ranging from 10^5 to 10^{12}.

Jing et al. 2015 [5] carried out experimental investigation on a solar chimney model with large gap-to-height ratios between 0.2 and 0.6. The experimental results show that the existing prediction method available in the literature over predicts the airflow rate for chimney geometry investigated in this work, especially for vertical solar chimney with large gap-to-height ratios. Better results, according to Jing et al 2015 [5], could be obtained by considering the pressure losses in the prediction. However, their experimental results show that an optimum gap-to-height ratio that maximizes the airflow rate in chimney is around the gap-to-height ratio of 0.5.

In recently published work, the effect of changing chimney gap on the mass flow rate of air at different chimney gaps ranged from 0.1 m to 0.5 m, have been reported by Hosien and Salim 2017 [6]. Results show that the mass flow rate increases sharply with increasing the chimney gap. As the gap increases from 0.1 to 0.5 m, the air flow rate increases from 0.04 to 0.18 kg/s. This means, as pointed by da Silva and Gosselin [1], that the gap of the chimney has a great effect on the natural ventilation flow rate. One can conclude that increasing chimney gap is more effective in increasing the air flow rate through the chimney. The consequences of increasing the chimney gap at constant other parameters is to reduce the friction losses inside the chimney channel and to increase the potential of buoyancy, thus the combination of these factors results in the increase of air flow rate.

The inclination of the solar chimney is another design parameter which, its effect on the solar chimney performance, has been investigated. Chen et al. (2003) [7] reported important experimental results pertaining to the inclination and the air gap of RTSC model, with one side heat flux. The experiments were carried out with 1:15 and 2:5 gap-to-height ratios. The best performance, in terms of maximum air flow, was achieved at an inclination around 45^o for 0.2 m gap and 1.5 m height. They experienced that the air flow is increased by 45% in the case of 45^o inclination compared to the vertical case. Mathur et al 2006a [8], have carried out similar experimental and mathematical investigation to that of Chen et al. 2003 [7], where

they investigated the influence of the ventilation due to variation in the gap-to-height ratio. Their calculation results showed disagreement compared to the experimental results. However, both, Chen et al. 2003 [7] and Mathur et al. 2006b [9] recommended 45^{o} inclination of the absorber, where the optimum ventilation was gained. Al-Kayiem and Yassen 2015 [10] investigated, experimentally, the natural convection in solar heated channels at range of inclinations from 30^{o} to 70^{o} for latitude of 4.39° N. There results demonstrated that the optimum inclination for solar air heater within 40^{o} to 50^{o} in tropical regions, which confirms the findings of Chen et al. 2003 [7] and Mathur et al 2006b [9]. In addition, Bassiouny and Korah 2009 [11] have numerically, using ANSYS software, showed that an optimum air flow rate was obtained at the chimney inclination between 45^{o}and 70^{o} for the latitude of 28.48.

The other design parameters draw the attention and investigated by many researchers is the inlet to the chimney. Spenser et al 2000 [12], through scaled solar chimney experimental model, revealed that larger inlet area to the solar chimney causing increase in the volume flow rate. Arce et al. 2009 [13] investigated the thermal performance of a ventilation solar chimney with a gap-to-height ratio of 0.07 under Mediterranean daylight and night time conditions for natural ventilation. Their experimental measurements showed that a solar chimney with side air inlet gave better thermal performance than that with bottom inlet.

Tan and Wong 2013 [14], through numerical simulation, studied the effect of many parameters on the flow and temperature on a solar chimney connected to the side of a room. Among the investigated parameter is the location of the side inlet from the room to the chimney. There simulation results are different compared with those obtained by Tan and Wong 2012 [15] performed experimentally on a class room. Lowering the inlet position to the middle position leads to significant increase in the output air velocity. The inlet position is mainly affect the air speed in the localized region around the solar chimney inlet. In the present work, it is found that the shape of the inlet also affects the air velocity, and the chimney performance, as well.

However, solar chimney geometries, inlet size and shape, construction materials and the surrounding weather conditions are all inter-dependent. Optimization of individual parameter at certain condition may not be optimum if combined with others. Since the solar is changing on a daily base, experimental investigations are not practical if they are considered as unique

analysis technique. Combined experimental measurements and computational simulations are essential and compliment to each other.

The literature revealed many investigations on various parameters that influencing the RTSC and the side wall SC; but it is clear that there is no attempt has been reported to study the effect of the inlet shape and its effect on the system performance. During preliminary numerical simulation of a RTSC, it has been realized that the inlet configuration causes change in the flow structure and the mass flow rate of air in the RTSC. Hence, this study was conducted with a specific object of investigating the inlet configuration effect on the performance of a RTSC. Four different inlet configurations have been identified and simulated numerically and experimentally at different solar irradiances.

2. PRINCIPLES OF RTSC AND PROBLEM FORMULATION

The main components of the RTSC system are a solar collector, and a chimney. The combination of the two parts represents natural solar updraft system. The collector converts the solar radiation to thermal energy in the absorber, and then kinetic energy in the flowing air. The collector consists of solar absorber surface and a transparent cover. They are inclined at an angle, θ and they are at a perpendicular distance, d apart. The inclination of the collector depends on the design of the RTSC, and it may be within a range of $0^o < \theta < 90^o$. Due to the distance between the cover and the collector, a pathway is created for air flow within environment of green house. The chimney part enhances the stack effect of the room air and/or the ambient air and to maintain the flow process. It may be in a rectangular or circular cross section. In the present work, the RTSC comprises of two identical halves of air solar collector installed over a roof of a room model, as shown schematically in Figure 1.

During sunny days, solar radiation penetrates through the transparent cover and heat up the absorber. The thermal energy transfers to the air in the pathway causing increase in the air temperature. The hot air rises and exits at the top while cooler air is drawn in from the collector inlet, providing a continuous air flow. Solar chimney has been widely used for power generation purposes; however there is still shortage on the effect of collector inlet configuration on the thermal process efficiency. Researcher had described seven principle factors which strongly affect the amount of solar radiation incident on a collector which are geographical location, site location of the collector, collector orientation, time of the day, time of the year, atmospheric condition, and collector design, which is referring to the

collector inlet configuration, or shape. This shape is critical in terms of the maximum allowed amount of air to flow from the surroundings to the collector with minimum resistance.

To investigate the effect of the collector inlet shape on the RTSC performance, four different inlet shapes have been selected in the present investigations. They could be described as:

Configuration 1: The length of the collector is larger than the transparent cover. The inlet cross section plane is vertical.

Configuration 2: The length of the collector and the cover are the same. The inlet cross section plane is inclined 45^o

Configuration 3: The length of the transparent cover is larger than the collector. The inlet cross section plane is horizontal.

Configuration 4: The shape of the transparent cover at the collector inlet is curved, similar to a case of installing water cutter.

3. EXPERIMENTAL INVESTIGATION

The layout of the present RTSC model is similar to the experimental model of Chungloo and Limmeechokchai 2009a [16] and 2009b [17] in Thailand, but with larger size, and different construction materials. The experimental RTSC is constructed utilizing the roof of a room that has 3.0 m length, 2.5 m width and 2.0 m height, where the roof is inclined at 45^o. The roof and the collector have 2 sides. Each collector on each side has 1.8 m long, from inlet to the outlet at the top of the collector. For the collector, corrugated zinc plate has been used to increase the effective collector area. The corrugated plate was painted black to maximize the absorptivity. The total area of the absorber plates in each side is 10.8 m^2, which is same as of the cover. To prevent heat loss from the back of the collector, heavy insulation was used behind the corrugated plate. Two layers of 10 mm-thick glass wool were glued to the back side of the plates. For the transparent cover, 5 mm-thick acrylic glass (Perspex) was used. Perspex was selected based on account of its moderate properties and easy handling than the glass. It also transmits up to 98% of visible light.

Following the recommendation of Khedari et al. [18] and Khedari et al. [19], the air gap between the collector and cover plate was set to 0.14 m. For convection heat transfer of air in passages, if the spacing is less than ~ 0.14 m, the frictional losses increase and create higher shear at the walls, which increase the resistance to the fluid flow and reduce the stack effect.

If the spacing is larger than ~ 0.14 m, the fully developed flow will be altered and large amount of ambient air in the core of the flow field will not gain heat from the surfaces causing the temperature rise of air is small and this reduces the collector performance, and consequently, the chimney performance reduces. The air gap between the absorber and cover plate was divided into three compartment sections using acrylic glass. Air flow up in the two sides of the collector and merge within Perspex made box at the top of the collector sides. The top wall of the merging box has a small inclination to enhance the flow of merged air towards the chimney base. The air, then, moves towards the base of the chimney, which was made of 152.4 mm diameter PVC pipe. The experimental set up is shown in Figure 3. The absorber plate was black painted at the time of experimental measurements. The absorber color looks gray due to the aging where the photo has been captured after two years of the fabrication.

However, the selection of the orientation of the experimental model is based on solar monitoring in the site. The measurement on east-west orientation and north-south orientation is shown figure 4. Each data point represents the mean measurements of two sides.

Then, accordingly, the top intersection line of the two collectors is oriented in north-south direction to permit the highest amount of solar radiation to be absorbed by the two collectors, oriented at east-west, during the day.

For constructing Configuration-1, the absorber plate has been extended by 0.1 m at both sides of the RTSC. Same corrugated zinc plate of the absorber, black painted, has been used for the extended plate and connected to the absorber plate by bolts and nuts. Configuration-2 is the standard shape inlet shape of the basically constructed RTSC, where the cover and absorber having the same length. Configuration-3 was made by fixing 0.1 m long Perspex sheet connected to the cover using bolts. For the construction of configuration-4, a standard PVC pipe of 0.14 m diameter has been cut into two equal halves to get 0.07 m diameter water gutter. They have been connected to both sides of the RTSC using bolts, nuts and metal supporting fixtures.

The surface temperature of absorber and cover were measured using J-type thermocouple with an accuracy of ±0.2°C, positioned in the middle of each of the three compartments, on both sides. Total of 12 thermocouples have been used for measuring both absorber and cover

temperatures. Three K–type probe thermocouples were installed inside the air merging box at the center of the air flow channel, where the air from both sides of the roof system and mixed together. All these thermocouples have been connected to a data logger type Fluke Hydra series II. Hot wire probe anemometer is used to measure the temperature and velocity of air at the base of the chimney pipe. The measurement of temperature and velocity of air captured and stored in the data logger starting from 10.00 am till 3.00 pm. A solarimeter was used to measure the direct and diffuse solar radiation.

4. NUMERICAL SIMULATION SETUP

The main aim of the numerical simulation in the present work is to allow flow visualization for qualitative evaluation, while the experimental measurements are providing quantitative evaluation. The experimental model of the RTSC was modeled in computational environment and the flow field and the thermal domain were simulated. Commercial ANSYS FLUENT software was utilized to conduct the 2D simulation. The inlet configuration was studied to determine the best configuration that would offer the highest mass flow rate of air into the system as the mass flow rate determined the amount of useful energy that the system could generate. The study involved the creation of a far field boundary to account for the ambient conditions which included the wind velocity and temperature. The incident solar radiation to the system was used to simulate the fluid flow and its field using the radiation model.

The nature of the problems determines the type of radiation model that may be more appropriate when deciding which radiation model to use are:

- Optical thickness.
- Scattering and emissivity.
- Semi-transparent media and specular boundaries.
- Non-grey radiation.
- Localized heat sources.
- Enclosure radiative transfer with non-participating media.

From the points above, the Discrete Ordinate (DO) radiation model was found to be the most suitable for the current study.

Adaptive secured mesh system was used for the present study. The structured mesh method was the Quad/Hex – mapped algorithm. The choice for this grid type was to take care of the irregular shapes relating to the joints between the surfaces of the system. When a system is under consideration requiring multi-block grids, the number of grids which is in thousands of blocks has automatically been generated. The number of blocks is large because of the complex topology. The use of a structured grid (SG), allows the alignment of the grid, resulting in locally a 1D flow. Hence, the numerical diffusion can be reduced, i.e., better accuracy is achieved. A Boundary Fitted Grid exactly matches the curved boundaries, and for complex Structure Domains (SDs) will consist of a set of blocks. The mesh generated for the system is 78,305 structured cells 157,797 faces and 79,493 nodes. Figure 5 shows concentric part of the meshed domain, surrounding the house model and inside the collector. However, in the present work, the far-field meshing option was adopted.

Proper boundary conditions are needed for a successful computational work. At the collector inlet, the temperature is specified as the ambient temperature with values as recorded in the experimental measurement; where at the chimney exit the outlet condition with zero static pressure is prescribed. The computation has been performed using the assumption of study, laminar flow with a uniform heat source added to the collector portion.

The buoyancy driven force is coupled with the energy and momentum equations and thus, makes the solution of the problem complex. In natural buoyancy driven flow calculations, the Boussinesq approximation is applied. The approximation states that the difference in density is to be neglected if it is small, except it appears in terms of being multiplied by acceleration due to gravity, g. The Boussinesq approximation is applicable when the difference in inertia is negligible but the acceleration due to gravity is much stronger. Boussinesq approximation models treat density as a constant value in all equations except in the buoyancy terms of the momentum equation.

$$\rho = \rho_0(1 - \beta\Delta T);\ where\ \beta\Delta T << 1 \quad (1.a)$$

$$\Delta P_{buoyancy} = \rho g H \beta \Delta T \quad (1.b)$$

The simulation proceeded with the CFD analysis via ANSYS FLUENT to solve the conservation equations 2 to 5. This CFD software is advanced solver technology to provide information on the streamline/velocity vector. Steady state, laminar assumptions have been employed. The set of conservation equations used by the software to solve the hydrothermal flow field are the conservation of mass, momentum and energy in two directions.

Continuity equation:

Under the assumption of incompressible, steady flow, the mass conservation, is

$$\frac{\partial(u)}{\partial x} + \frac{\partial(v)}{\partial y} = 0 \qquad (2)$$

Momentum equations:

Under the assumption of constant pressure at any point in the cross section perpendicular to the flow in the channel,

$$\rho\left(u\frac{\partial u}{\partial x} + v\frac{\partial u}{\partial y}\right) = -\frac{\partial p}{\partial x} + \mu\left(\frac{\partial^2 u}{\partial x^2} + \frac{\partial^2 u}{\partial y^2}\right) + S_{b,x} \qquad (3)$$

$$\rho\left(u\frac{\partial v}{\partial x} + v\frac{\partial v}{\partial y}\right) = \mu\left(\frac{\partial^2 v}{\partial x^2} + \frac{\partial^2 v}{\partial y^2}\right) + S_{b,y} \qquad (4)$$

Boissenisq approximation implies that:

$$S_{b,x} = (\rho - \rho_\infty) g_x$$

$$S_{b,y} = (\rho - \rho_\infty) g_y$$

Energy Equation:

Under the assumption that the temperature rise in the system is not high, thermal air properties are justify to be considered constants, then, the conservation of energy, is

$$\rho C_p\left(u\frac{\partial T}{\partial x} + v\frac{\partial T}{\partial y}\right) = k\left(\frac{\partial^2 T}{\partial x^2} + \frac{\partial^2 T}{\partial y^2}\right) \qquad (5)$$

Where u represents the flow velocity component in axial direction; v represents the traverse flow component; p is the local static pressure; ρ and ρ_∞ are density and reference density, while T is the temperature and μ and k are the viscosity and thermal conductivity of air, respectively.

The temperature domain is variable in both x and y directions. No turbulence model is needed to be considered in the simulation, since the flow is at low velocity, and it is laminar. The 2-D assumption is justified since the width to the gap ratio 3.0/0.14 = 21.4), is very large, where the width is 3.0 m and the gap is 0.14 m.

The iteration continues until the error of all the equations converges into minimum values. A typical run takes four to six hours in a desktop computer.

5. RESULTS AND DISCUSSION

The roof RTSC is simulated computationally and experimentally. The numerical simulation is assumed 2D and this assumption is justified as the width-to-gap ratio is 21.4 which very large. Through the simulation results, the velocity vector profiles of the four inlet configurations have been produced and analyzed. Each inlet configuration have been subjected to measurements repeatability of five days, and the mean is considered. Experimentally, the velocity and temperature have been measured at various locations in the air path inside the collector. By this raw measurements data, the mass flow rate could be evaluated, and then the collector performance could be predicted and compared for the four inlet configurations.

5.1. VALIDATION OF NUMERICAL PROCEDURE

Prior to present and discuss the results, the numerical procedure has been validated through comparison of the system performance and temperature as predicted numerically and measured experimentally. Figure 6 presents the predicted and simulated performance indicator of the RTSC, which becomes the heat gain by air if multiplied by the specific heat, using the data of the basic inlet configuration-2. The temperature parameter is representing the air temperature rise at the chimney inlet above the ambient temperature. The mass flow rate is evaluated using the measured velocity at the chimney base and chimney pipe area, with state equation for the air density. The same experimental mean parameters have been used as input to the simulation at each particular time. In terms of performance behavior, the trends of both, experimental and numerical are similar over the measurement time, from 10.00 am to 3.00 pm. Generally, the predicted simulation results of the performance indicator are bit higher than the experimentally measured results. The mean percent of relative error is 5.86% and the maximum is 7.14%, which demonstrates good agreement.

Another comparison has been conducted to validated the computational procedure and justify the simulation results through air temperature comparison, as depicted in Figure 7. The figure display the results of air temperature measured at the base of the chimney pipe starting from early morning, where the solar radiation almost equal to zero. The recorded solar radiation in during the experiments is input as boundary condition to the simulation. The predicted air temperature at the top of the collector is extracted from the simulation. The measurements and the simulation results have similar trends, where, air temperature is increasing as the solar radiation increases. The simulation over predicted the temperature of air at the chimney base with small margin of around 1.5% as a mean of relative error.

5.2. ANALYSIS OF INLET CONFIGURATION RESULTS

The results in this section would be presented simultaneously, as measured experimentally and predicted numerically, for each configuration. The velocity vector contours at the collector inlet has been used to characterize the configuration, while the velocity at 0.5 m above the chimney base is adopted to compare between the experimental and numerical results of each configuration. The simulation results presented in the analysis, as velocity vectors, are in the west side of the collector.

5.2.1. Numerical analysis

Analysis of Configuration 1

In this configuration, the cover and the absorber have same length and the inlet cross section is vertical. The velocity vector profile is shown in Figure 8 as pictorial view to visualize the flow field at the inlet and inside the collector. Air particles are concentrated at the inlet and moves up in the collector with non-uniform profile. It is clear that air particles approach the inlet from all directions surrounding the inlet. On the upper surface of the cover, as well as near the room wall, the particles are moving parallel to the surfaces and accelerate as approaching the inlet. After short distance from the inlet, air particles near the absorber plate accelerated faster due to the energy gained from the hot absorber. The particles near the absorber surface move with higher velocity causing non uniform velocity profile across the section between the absorber and the cover.

The velocity profile at the velocity reference section in the chimney is presented in Figure 9. The mean velocity is around 1.47 m/s, while the maximum is 2.47 m/s.

Analysis of Configuration 2

Configuration 2 has cover plate longer than the absorber plate. The inlet cross section is inclined by 45^{o} with vertical plane. The velocity vector profile, of configuration 2, depicted in Figure 10, shows that air particles are approaching the collector inlet from all the outside directions. Velocity of air layers close to the absorber plate are higher compared to the other layers. However, the thermal energy transfer from the absorber to the air particles is sufficient to attaining good velocity and move up to the mixing chamber at the top of the collector.

The velocity profile at the velocity reference section in the chimney is shown in Figure 11. The maximum velocity is 2.11 m/s and the mean velocity is 1.18 m/s. the non-uniform velocity distribution is due to the fact the flow from the two sides of the SC is not identical. One side is receiving solar radiation larger than the other side.

Analysis of configuration 3

In configuration 3, the cover plate is longer than the absorber plate. The inlet cross section plane is horizontal. The velocity vector profile obtained from the simulation is presented in Figure 12. The performance of this configuration is the lowest compared to the other configurations. Air particles above the cover are gaining heat and accelerate towards the inlet of the collector. The particles accelerate from all directions surrounding the inlet and start to gain heat immediately as they are in the flow passage. Particles are gaining heat from both, the cover and the absorber plate. Motion is higher near the absorber compared to the close layers to cover.

At the velocity reference section in the chimney base, the mean velocity is about 0.82 m/s, while the maximum velocity is around 1.03 m/s. the predicted velocity profile is shown in Figure 13

Analysis of configuration 4

This configuration was considered assuming rain water collection from the roof by attaching gutter to the cover plate. The velocity vector profile of the air, shown in Figure 14, demonstrates that the particles approaching the inlet from underneath have larger velocity compared to the particles coming from the upper region. The air flow velocity is increased at the smallest inlet cross section and then decelerates as the area increase. After gaining thermal energy from the cover and the absorber, the flow accelerates towards the outlet of the collector. The shape of the gutter resists the motion of the particles.

At the chimney velocity reference section, the mean velocity is 1.11 m/s and the maximum is 1.89 m/s. The non-uniformity of the velocity profile, shown in Figure 15, is more obvious compared to the other cases.

The summary of the simulation results is presented in Figure 16 and table 2. The figure displays the velocity profiles of the four inlet configurations as predicted at the velocity reference section in the chimney pipe. The profiles are not identical due to non-uniform solar absorption by the absorbers on the two sides of the roof. Consequently, the flow in the two side of the collector is not similar. The results revealed that configuration 1, with vertical inlet cross section, is possessing optimal performance as it lead to highest flow rate.

An interesting phenomenon has been realized from the flow visualization by CFD velocity vectors that explain the reason behind the various performances of the inlet configurations. In all cases of inlet configurations, air particles are mainly supplied to the collector inlet from the upper surface. It is contradictory to the expectation that as the particles receiving heat from top of the cover, they move up as a result of the natural convection heat transfer. What is happening that the particles are moving parallel to the cover with accelerated velocity and turn down to inter inside the collector. The solar chimney is operating as a suction tool and imposes kinetic energy before the particles start to gain heat from the absorber plate. This is a reasonable justification for the low performance of the collector with inlet configuration 3, where the particles need to turn by 180^{o} to move from the upper surface of the cover and inter inside the collector. Also, it is the reason why configuration 1 resulted in the best performance, where the particles move shorter distance on the upper surface of the cover and turn by lower angle to inter the collector.

5.2.2. Experimental analysis

During each measurement, the solar radiation on horizontal plane, the ambient temperature and the humidity have been recorded on hourly base. The trend of the wind speed is almost sustained within a range of 0.5 to 1.5 m/s. it is occasionally happening that the wind speed exceeding 2.0 m/s. For this low variation in the wind speed, the losses due to convection heat transfer could be assumed fixed, as the convection heat transfer is varying within the range of 4.3 to 7.3 W/m^2·K during the experimental measurement time. The convective heat transfer from the canopy to the ambient might be calculated using equation 1 (Duffie and Beckman 2013 [20]).

$$h_{c-wind} = 2.8 + 3.0\, V_w \quad (1)$$

The record of ambient temperature is presented in figure 17. Each line is refereeing to mean ambient temperature of five days, for each configuration. Generally, the ambient temperature in the morning is low, at value of 26±1^{o}C. The ambient temperature is increasing and reaching the maximum values during the day at the high solar radiation period in the afternoon till the sunset. The maximum ambient temperature is around 35±1.5^{o}C. After the sunset, the ambient temperature is reducing gradually.

The recorded solar radiations, as mean of five days for each configuration, are shown in figure 18. The trend of solar radiation is similar for all configurations. The maximum, as commonly practiced, is around 2.00pm. Cases of less values than the average is due to occasional cloud. The mean maximum recorded solar radiations are 937, 975, 930, 956 w/m^2 for configurations, 1, 2, 3 and 4, respectively.

The performance of RTSC could be evaluated using suitable indicator for the ability to convert the solar radiation to updraft driving force. This indicator is representing temperature rise of the generated air mass flow rate by the natural convection heat transfer, $\dot{m}\,\Delta T$. The mass flow rate could be determined from the measured flow rate, and ΔT from the measured temperatures at the ambient conditions and at the velocity reference section in

the chimney. The results for the performance indicator variation with time are shown in Figure 19. The best performing configuration over the entire measurement period is configuration 1. Slightly lower performing is configuration 2. A noticeable difference is realized when comparing the results of configurations 3 and 4. A considerable reduction in the performance is clear in the case of collector with inlet configuration 3.

However, comparison of the maximum and mean velocity values is compiled in Table 2. The best performing is configuration 1, while the lowest is configuration 3. Comparison between the experimental and numerical velocity results demonstrates that the average of the maximum relative percentage of error is around 7.6%.

6. CONCLUSIONS

Four different configurations of air inlet to the solar collector, as part of a roof top solar chimney, have been investigated experimentally and numerically. Results revealed that inlet configuration to the collector is influencing the performance of the system. Inlet configuration with vertical cross section provided the best performance in terms of highest velocity and highest performance indicator. Interesting finding from the CFD visualization exposes that most of the air particles inter to the collector are directed from top region. When the inlet cross section is employed as horizontal, the performance of the collector is reduced by 84% compared to the vertical inlet setting, at 1.00pm.

It is then recommended to design the inlets of free convection solar systems, similar to the RTSC, with inlet orientation that allows as much as air particles to flow in the collector passage from the top portion of the inlet structure. Such system are the air solar collectors, the inclined solar chimney and the indirect solar dryers.

ACKNOWLEDGMENT

The authors would like to acknowledge Universiti Teknologi PETRONAS for the financial and logistic support to conduct the works under the internal research grant, STIRF 09/07.08. In particular, Dr Sreejaya and Dr Aja are expressing their thankful remarks to UTP for the financial support of their PhD study under the Graduate Assistance (GA) scheme.

REFERENCES

[1] A.K. da Silva, L. Gosselin, Optimal geometry of L and C-shaped channels for maximum heat transfer rate in natural convection, Int. J. Heat Mass Transfer 48 (2005) 609–620.

[2] K.S. Ong A mathematical model of solar chimney. Renewable energy 28, (2003a). 1047-1060.

[3] K.S. Ong and C.C. Chow. Performance of solar chimney. Solar Energy 74, (2003b). 1-17

[4] B. Zamora, A.S. Kaiser. Optimum wall-to-wall spacing in solar chimney shaped channels in natural convection by numerical investigation. Applied Thermal Engineering 29, 2009. 762–769

[5] Haiwei Jing, Zhengdong Chen and Angui Li, Experimental study of the prediction of the ventilation flow rate through solar chimney with large gap-to-height ratios. Building and Environment 89, 2015. 150-159.

[6] M.A. Hosien, S.M. Selim. Effects of the geometrical and operational parameters and alternative outer cover materials on the performance of solar chimney used for natural ventilation. Energy and Buildings 138 (1) 2017, Pages 355–367.
http://dx.doi.org/10.1016/j.enbuild.2016.12.041

[7] Chen Z.D., Bandopadhayaya P., Halldorssonb J., Byrjalsenb C., Heiselbergb P., Lic Y., (2003) An experimental investigation of a solar chimney model with uniform wall heat Flux, Building and Environment 38, 893–906.

[8] Mathur, J., Mathur S., and Anupma (2006a). Summer performance of inclined roof solar chimney for natural ventilation, Energy and Buildings 38, 1156-1163.

[9] Mathur, J., Bansal N.K., Mathur S., Jain M. and Anupma (2006a). Experimental investigations on solar chimney for room ventilation, Solar Energy Volume 80, issue 8, pages 927-935.

[10] Al-Kayiem, H., H., Yassen, T. A., 2015. On the natural convection heat transfer in a rectangular passage solar air heater. Solar Energy 112, 310-318.

[11] R. Bassiouny and N. S. A. Korah, "Effect of solar chimney inclination angle on space flow pattern and ventilation rate, Energy and Buildings 41, pp. 190-196, 2009.

[12] Spencer, S., Chen Z.D., Li, Y. and Haghighat, F. Experimental investigation of a solar chimney natural ventilation system. In Air Distribution in Rooms, Proceedimgs of the 7th International Roomvent Conference, Reading, UK, 9-12 July 2000. Pp. 813-818.

[13] Arce J, Jimenez MJ, Guzman JD, Heras MR, Alvarez G, Xaman J. Experimentalstudy for natural ventilation on a solar chimney. Renewable Energy 34. 2009, 2928-34.

[14] Tan, A.Y.K. and Wong, N.H. Parameterization studies of solar chimney in the tropics. Energies 6, 2013.

DOI:10.3390/en6010145

[15] Tan, A.Y.K.; Wong, N.H. Natural ventilation performance of classroom with solar chimney system. Energy and Buildings 53, 2012. 19-27.

[16] S. Chungloo and B. Limmeechokchai, (2009a), Application of passive cooling systems in the hot and humid climate: The case study of solar chimney and wetted roof in Thailand, Building and Enviornment 42 (9), pages 3341-3351.

[17] Sudaporn Chungloo, Bundit Limmeechokchai, (2009b),The utilization of cool ceiling chimney with roof solar chimney in thailand: the experimental and numerical analysis, Renewable Energy 34, 623-633J.

[18] J. Khedari, et al., Ventilation impact of a solar chimney on indoor temperature fluctuation and air change in a school building, Energy and Buildings 32, pp. 89-93, 2000.

[19] J. Khedari, et al., Field study of performance of solar chimney with air-conditioned building, Energy 28, pp. 1099-1114, 2003.

[20] J.A. Duffie, W.A. Beckman, Solar Engineering of Thermal Processes, ISBN: 9781118671603, Wiley online library , 2013

DOI: 10.1002/9781118671603

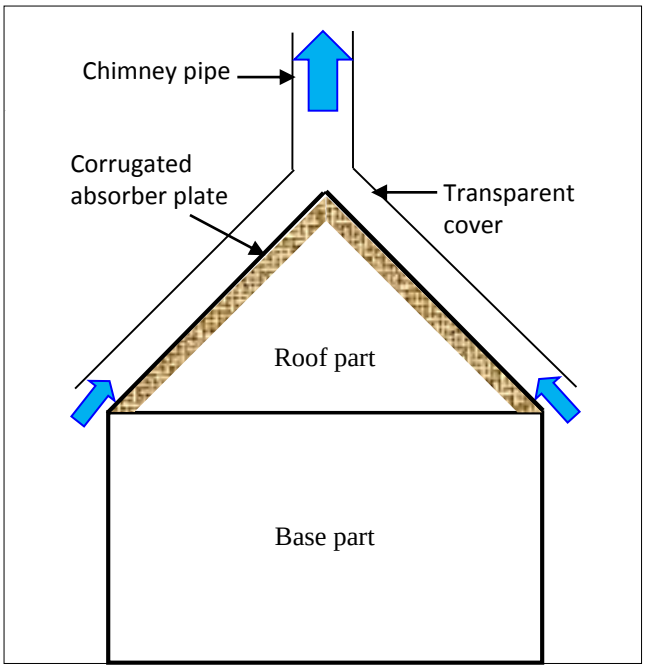

Figure 1: Schematic diagram of the identical two sides RTSC

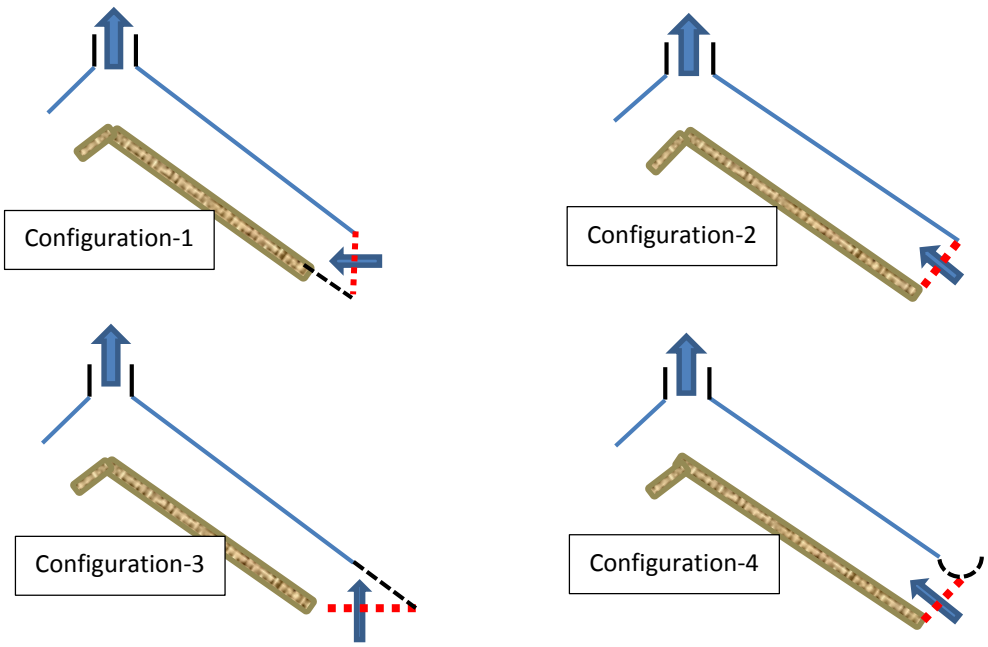

Figure 2: Four different inlet configurations investigated experimentally and numerically.

Figure 3: Experimental model of the identical two sides RTSC.

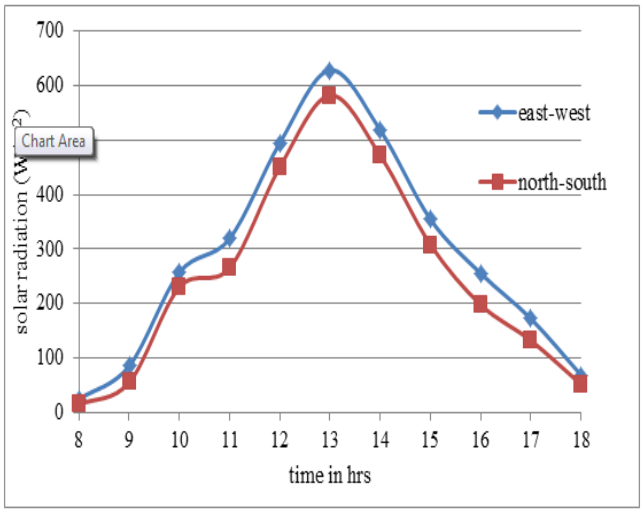

Figure 4. Mean of five days measured solar radiation on east-west side and north-south side oriented roofs.

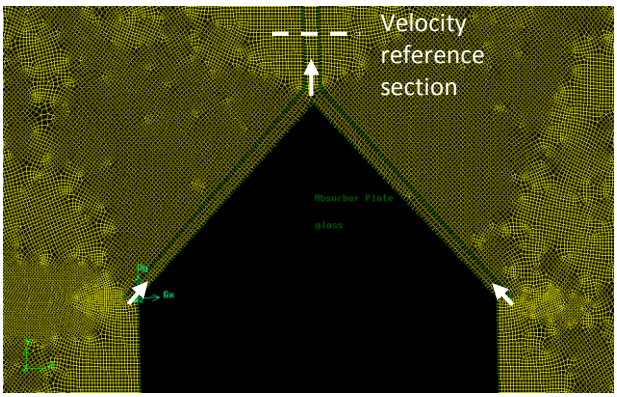

Figure 5: Concentric view of the meshing of RTSC in the 2-D model.

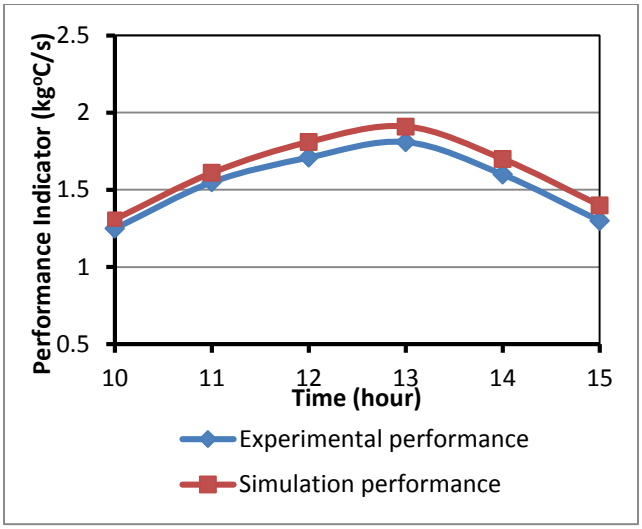

Figure 6: Performance results of the roof top solar chimney as measured experimentally and predicted numerically over the test period from 10.00am to 3.00pm; configuration 2.

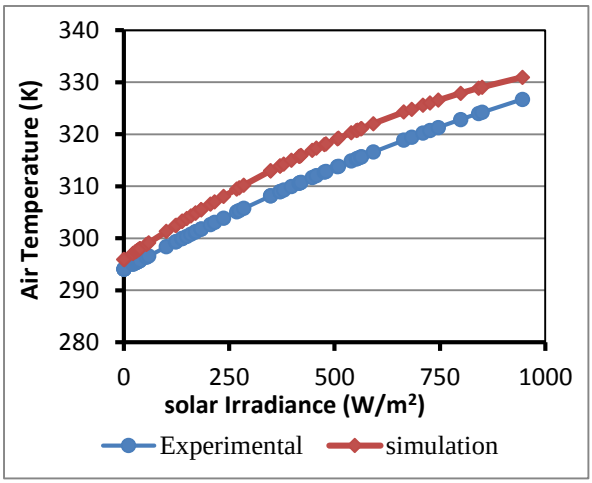

Figure 7: Measured and simulated air temperature at the chimney base, for configuration-2 at various solar irradiances.

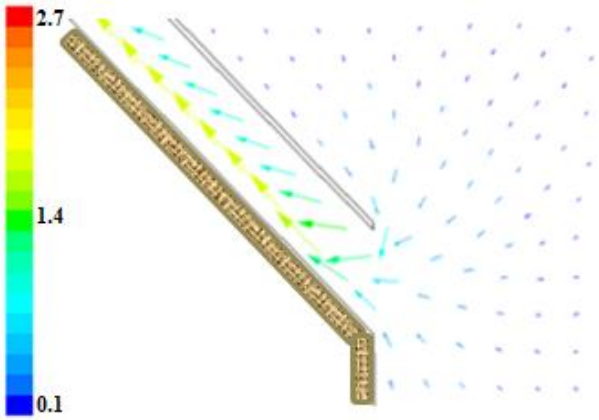

Figure 8: Simulation results as velocity vector profile of Configuration 1, (m/s)

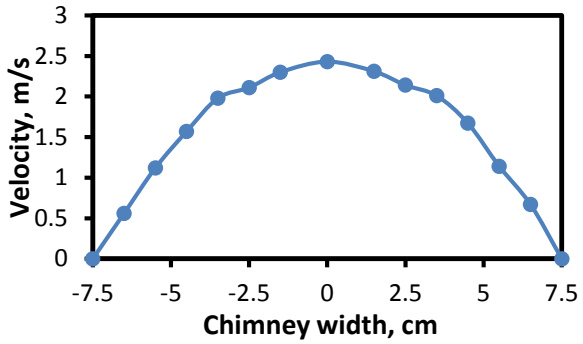

Figure 9: Predicted velocity profile at the velocity reference section in the chimney (collector inlet configuration 1, at 1.00pm).

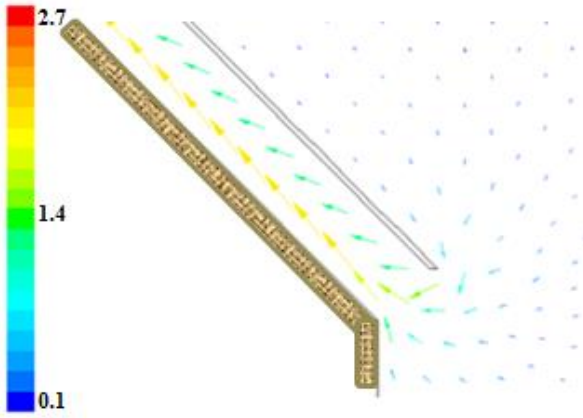

Figure 10: Simulation results as velocity vector profile of configuration 2, (m/s)

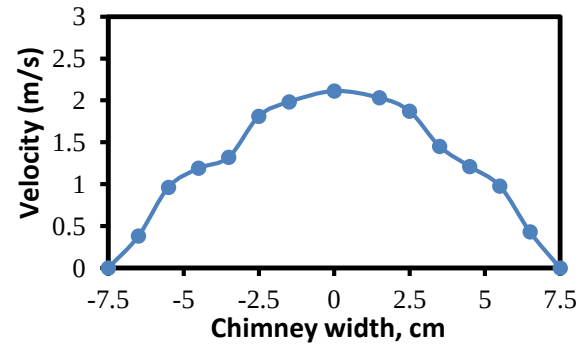

Figure 11: Predicted velocity profile at the velocity reference section in the chimney (collector inlet configuration 2, at 1.00pm)

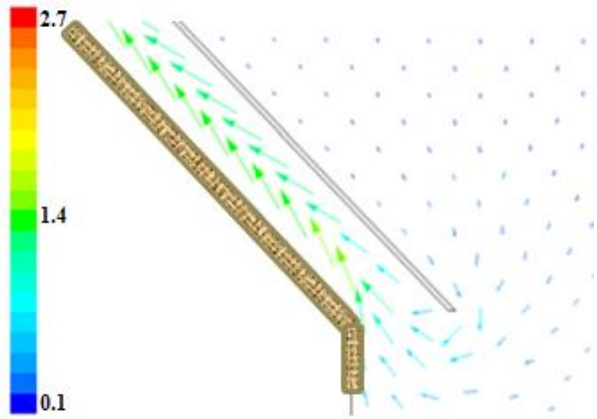

Figure 12: Simulation results as velocity vector profile of configuration 3, (m/s).

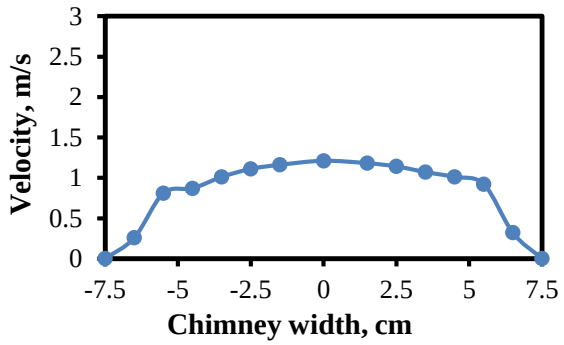

Figure 13: Predicted velocity profile at the velocity reference section in the chimney (collector inlet configuration 3, at 1.00pm)

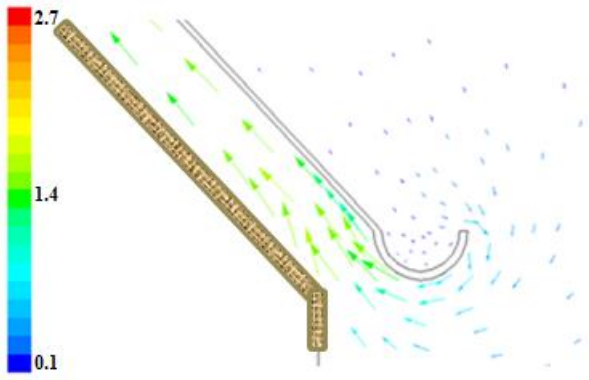

Figure 14: Simulation results as velocity vector profile of configuration 4, (m/s).

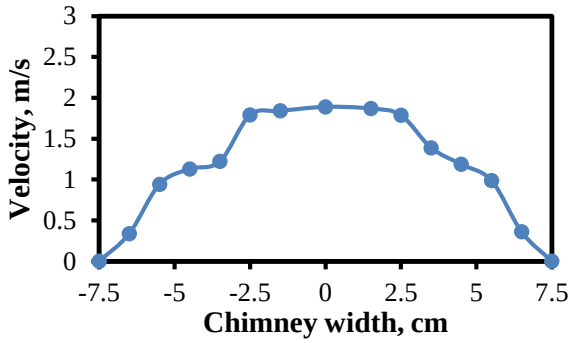

Figure 15: Predicted velocity profile at the velocity reference section in the chimney (collector inlet configuration 4, at 1.00pm).

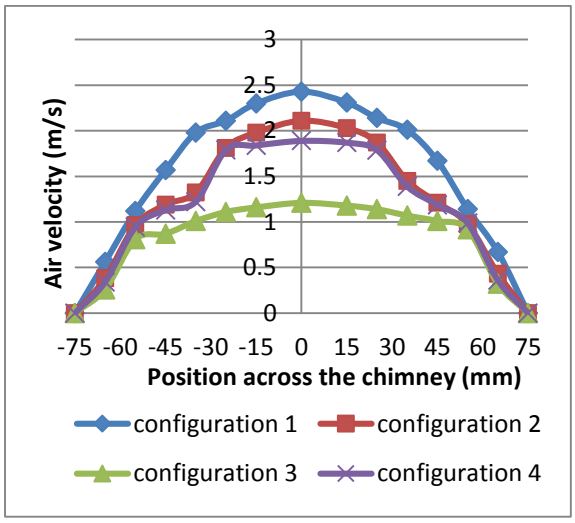

Figure 16: Numerically predicted velocity profiles at the velocity reference section in the chimney pipe for the four inlet configurations.

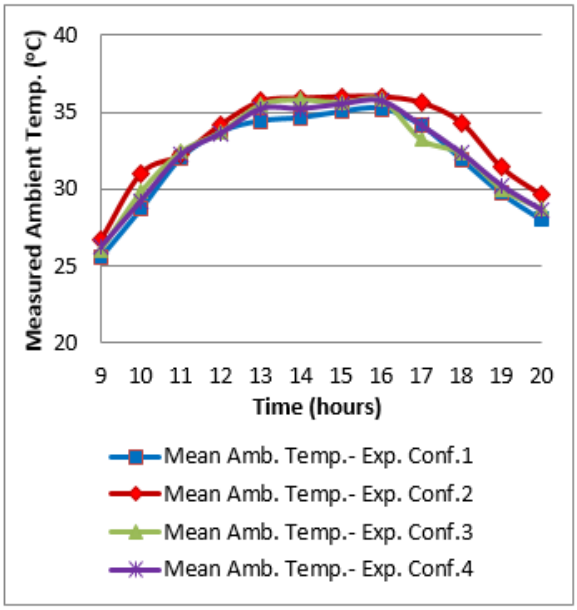

Figure 17: Measured ambient temperatures during the experiments of each configuration. (Results of each configuration is the mean of the five days of experiments).

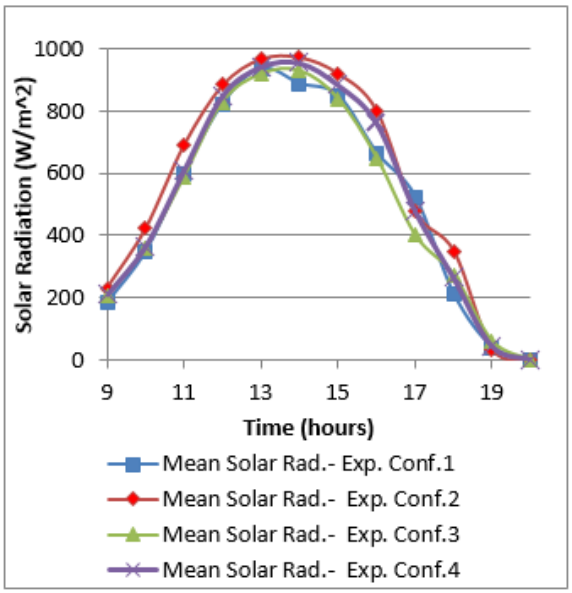

Figure 18: Measured solar radiation during the experiments of each configuration. (Results of each configuration is the mean of the five days of experiments).

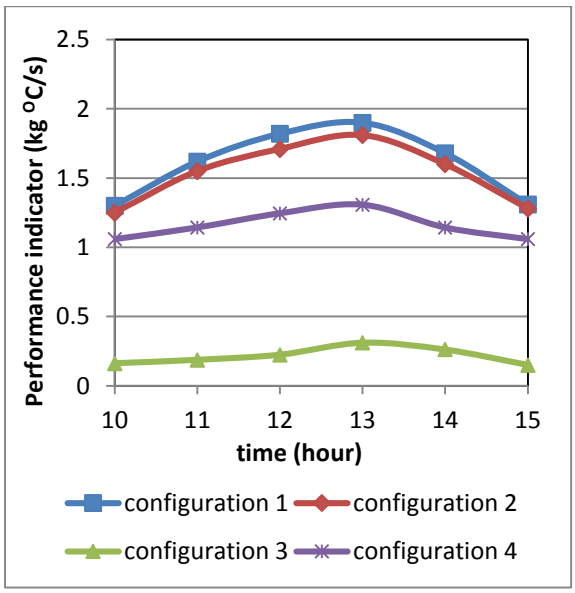

Figure 19: Experimental results of the performance indicator of four inlet configurations.

Table 1: Boundary conditions based on the settings on FLUENT.

Component	**Boundary Type**	**Value**
Absorber plate	wall	$T_{absorber}$ = 322 K
Transparent Cover	wall	T_{cover} = 310 K
Back insulator	wall	q = 0 W/m^2, perfect insulation
Chimney wall	wall	q = 0 W/m^2, perfect insulation
Fluid	air	Boussinesqi approximation
Greenhouse inlet	inlet	Velocity = 0.05 m/s
Chimney exit	Pressure outlet	Gauge pressure = 0 Pa

Table 2: Numerically predicted and experimentally measured velocities, at the velocity reference section in the chimney, of four different inlet configurations.

configuration	Numerical		Experimental	Percent of error (%)
	Max vel. (m/s)	Mean vel. (m/s)	Mean vel. (m/s)	
1	2.43	1.47	1.51	2.65
2	2.11	1.18	1.31	9.90
3	1.21	0.80	0.92	13.0
4	1.89	1.12	1.18	5.08